Quasicompactons in inverted nonlinear photonic crystals

Yongyao Li,[1,2,*] Boris A. Malomed,[3,4] Jianxiong Wu,[1,5] Wei Pang,[6] Sicong Wang,[2] and Jianying Zhou[2,†]

[1]*Department of Applied Physics, South China Agricultural University, Guangzhou 510642, China*

[2]*State Key Laboratory of Optoelectronic Materials and Technologies, Sun Yat-sen University, Guangzhou 510275, China*

[3]*Department of Physical Electronics, School of Electrical Engineering, Faculty of Engineering, Tel Aviv University, Tel Aviv 69978, Israel*

[4]*ICFO-Institut de Ciencies Fotoniques, Mediterranean Technology Park, E-08860 Castelldefels (Barcelona), Spain*

[5]*Department of Electrical and Computer Engineering, University of Toronto, Toronto, Ontario M5S-3G4, Canada*

[6]*Department of Experiment Teaching, Guangdong University of Technology, Guangzhou 510006, China*

(Received 20 August 2011; published 24 October 2011)

We study large-amplitude one-dimensional solitary waves in photonic crystals featuring competition between linear and nonlinear lattices, with minima of the linear potential coinciding with maxima of the nonlinear *pseudopotential*, and vice versa (*inverted nonlinear photonic crystal*s, INPCs), in the case of the saturable self-focusing nonlinearity. Such crystals were recently fabricated using a mixture of SU-8 and Rhodamine-B optical materials. By means of numerical methods and analytical approximations, we find that large-amplitude solitons are broad sharply localized stable pulses (*quasicompactons*, QCs). With the increase of the total power, P, the QC's centroid performs multiple switchings between minima and maxima of the linear potential. Unlike cubic INPCs, the large-amplitude solitons are mobile in the medium with the saturable nonlinearity. The threshold value of the kick necessary to set the soliton in motion is found as a function of P. Collisions between moving QCs are considered too.

DOI: 10.1103/PhysRevA.84.043839 PACS number(s): 42.65.Tg, 42.70.Qs, 05.45.Yv

I. INTRODUCTION AND THE MODEL

Photonic and matter waves propagating under the combined action of linear and nonlinear lattice (LL and NL) potentials exhibit a number of dynamics [1]. In particular, solitons in such media is a topic of considerable current interest, see recent review in Ref. [2] and original works in Refs. [3,4] devoted to the studies of 1D solitons. Other works were dealing with solitons [5,6] and localized vortices [7] in 2D versions of such systems, which represent, in particular, photonic crystal fibers [8] and 2D photonic crystals [9] made of nonlinear materials. The evolution of solitons in these systems obeys the nonlinear Schrödinger equation (NLSE), in which the LL and NL are represented, respectively, by a usual periodic potential and by a periodic *pseudopotential* [2,10], which is induced by a spatially periodic modulation of the local nonlinearity coefficient. In optics, the NL represents the mismatch between the nonlinearity of the host material and the stuff filling voids of the photonic-crystal-fibers structure, which may be air, another solid material [11], or a liquid crystal [12]. The same model, in the form of the Gross-Pitaevskii equation, applies to matter waves in a Bose-Einstein condensate (BEC), which is trapped in a combination of a linear periodic potential, created by an optical [13] or magnetic [14] lattice, and a pseudopotential lattice, that may be induced by a periodic modulation of the local nonlinearity provided by a properly patterned [2] external magnetic [15] or optical fields [15].

Recently, a combination of *competing* π-out-of-phase-juxtaposed LL and NL, with maxima of the refractive index coinciding with minima of the local strength of the self-focusing nonlinearity and vice versa, was considered in several works [17–19]. This medium may be naturally called an *inverted nonlinear photonic crystal* (INPC). It was reported that INPCs could be fabricated by means of the technique based on direct laser writing in silica [20]. It was also predicted that a similar setting can be created in a virtual form, using the electromagnetically induced transparency acting on dopant atoms periodically distributed in a passive matrix [19]. Due to the competition between the LL and NL, solitons in INPCs may feature specific power-dependent properties, such as double symmetry breaking [19]. While previous studies of INPCs were dealing with theKerr (cubic) nonlinearity, in this work we consider solitary waves in the system with saturable nonlinearity, which occurs in various optical media. The extension of the analysis for this nonlinearity is natural, while solitons in INPCs feature the strong sensitivity to the power.

First, we propose an experiment setup to realize an INPC with a saturable nonlinearity. Recent works reported the creation of resonantly absorbing waveguide arrays and *imaginary-part photonic crystals* that feature a spatially periodic modulation of the absorption coefficient, built on the basis of the SU-8 polymer (a commonly used transparent negative photoresist) doped with Rhodamine B (RhB, a dye featuring saturable absorption) [21,22]; see Fig. 1 for a schematic setup.

A similar pattern can be used for our purposes. In the paraxial approximation, the light propagation in the array obeys the spatial-domain NLSE for the local amplitude of the electromagnetic field, $u(z,x)$, where z and x are the propagation distance and transverse coordinate:

$$iu_z = -\frac{1}{2k}u_{xx} - \frac{(k_0\delta n + i\alpha/2)R(x)}{1+|u|^2}u. \tag{1}$$

Here, $R(x)$ is the array's structure function, which is to be taken as per Fig. 1(a), $k = k_0 n$, where $n = 1.62$ is the refractive index of pure SU-8, $k_0 = 2\pi/\lambda$, and λ is the wavelength of light in vacuum. Further, α and δn are the absorption coefficient and

*yongyaoli@gmail.com
†stszjy@mail.sysu.edu.cn

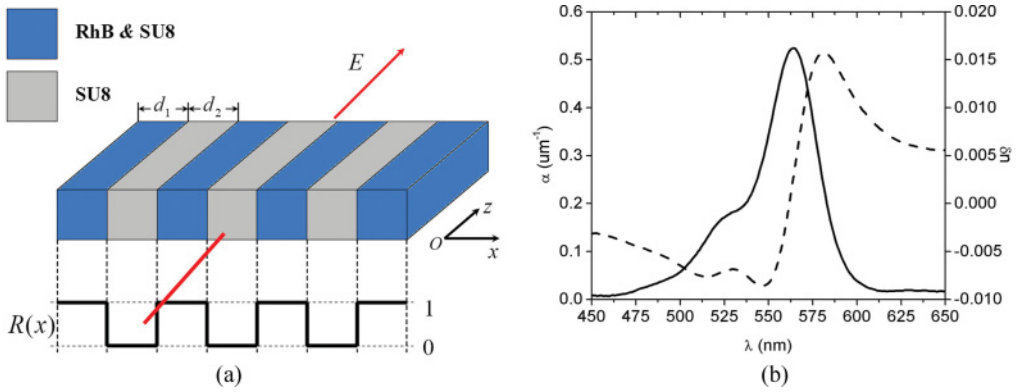

FIG. 1. (Color online) (a) The 1D nonlinear photonic crystal, with the blue and gray areas depicting the nonlinear and linear stripes, respectively. (b) The wavelength dependence of the absorption coefficient and refractive-index variation, α and Δn (solid and dashed lines, respectively) in the SU-8–RhB mixture.

refractive index difference between the SU-8–RhB mixture and pure SU-8, respectively, which are coupled by the Kramers-Kronig relation, and are plotted versus λ in Fig. 1(b) [22]. According to experimental data [22], in the relevant range of far blueshift from the absorption peak ($\lambda \approx 460$ nm), $\alpha/2 \simeq (1/20)k_0\,|\delta n|$, which allows one to neglect the dissipative term in Eq. (1), simplifying it to

$$iu_z = -\frac{1}{2}u_{xx} + \frac{V(x)}{1+|u|^2}u, \tag{2}$$

where k was removed by rescaling of x, and $V(x) \equiv -(k_0\delta n)\,R(x)$.

In the system under consideration, light experiences strong saturable self-focusing induced by RhB in the mixed material, while the nonlinearity of pure SU-8 is negligible. On the other hand, the refractive index of the mixture is smaller than in pure SU-8, i.e., $\delta n < 0$ at $\lambda = 460$ nm, hence, function $V(x)$ in Eq. (2) takes positive values, and the waveguide array meets the condition of the π phase shift between the spatial modulations on the linear and nonlinear local characteristics of the medium, thus realizing the INPC with the saturable nonlinearity.

The objective of this work is to study the existence, stability, mobility, and interactions of solitons in the INPC model based on Eq. (2). In Sec. II, we study properties of the solitons by means of numerical simulations and analytical approximations. It will be demonstrated that they feature sharp localization, i.e., a quasicompacton (QC) shape. Following the increase of the total power, P, the QC switches its position between maxima and minima of the linear refractive index. In Sec. III, we study mobility of the QCs, imposing the phase tilt onto them, i.e., suddenly multiplying the wave form by $\exp(i\eta x)$. A critical tilt (alias *kick*), $\eta_c(P)$, beyond which the compacton starts to move, is found. The dependence $\eta_c(P)$ features variations with the same period in P as the above-mentioned switching of the quiescent solitons. Collisions between moving compactons are also studied in Sec. III by means of direct simulations. The paper is concluded by Sec. IV.

II. QUASICOMPACTONS: NUMERICAL AND ANALYTICAL RESULTS

A. Numerical simulations

Modulation function $V(x)$ in Eq. (2) corresponding to Fig. 1 is a piecewise-constant one, of the Kronig-Penny type. In this paper, we approximate $V(x)$ by the first term of its harmonic decomposition, assuming that contributions of higher harmonics are negligible for sufficiently broad solitons:

$$V(x) = (V_0/2)\,[1 - \cos(2\pi x/d)]\,, \tag{3}$$

where d and $V_0 > 0$ are the modulation period and depth. The scaling is set by fixing $d \equiv 20$, which leaves V_0 as a free parameter. In this section, we present numerical results for $V_0 = 0.02, 0.03$, and 0.04, which adequately illustrate the generic situation. Below, we focus on solitons with a sufficiently large amplitude, as for small amplitudes the truncated expansion of the saturable nonlinearity amounts to the previously studied Kerr model [17–19].

Typical numerical results for solitons solution at different values of the total power, $P = \int_{-\infty}^{+\infty} |u(x)|^2 dx$, are displayed in Fig. 2. The stationary profiles, presented in Figs. 2(a)–2(c), were generated by dint of the the imaginary-time-propagation method [23]. It is concluded that the profiles are strongly localized, making the solitons QCs (quasicompactons) [a solution fully localized within a finite (*compact*) interval of y is usually called a compacton [24,25]]. On the other hand, the soliton broadens with the increase of P. At relatively small values of the total power, e.g., $P = 400$, the center of the soliton is located at a minimum of $V(x)$ [Fig. 2(a)]; then, at $P = 800$ [Fig. 2(b)], the position of the soliton is switched to a maximum of $V(x)$, and at $P = 2000$ it switches back to the minimum [Fig. 2(c)].

To quantify power-dependent properties of the solitons, we define the center-of-mass coordinate and average width of the soliton as follows:

$$\begin{aligned} X_{\rm mc}(P) &= P^{-1}\int_{-\infty}^{+\infty} x|U(x,P)|^2 dx, \\ W_{\rm a}(P) &= P^{-1}\int_{-\infty}^{+\infty} (x - x_{\rm mc})^2|U(x,P)|^2 dx, \end{aligned} \tag{4}$$

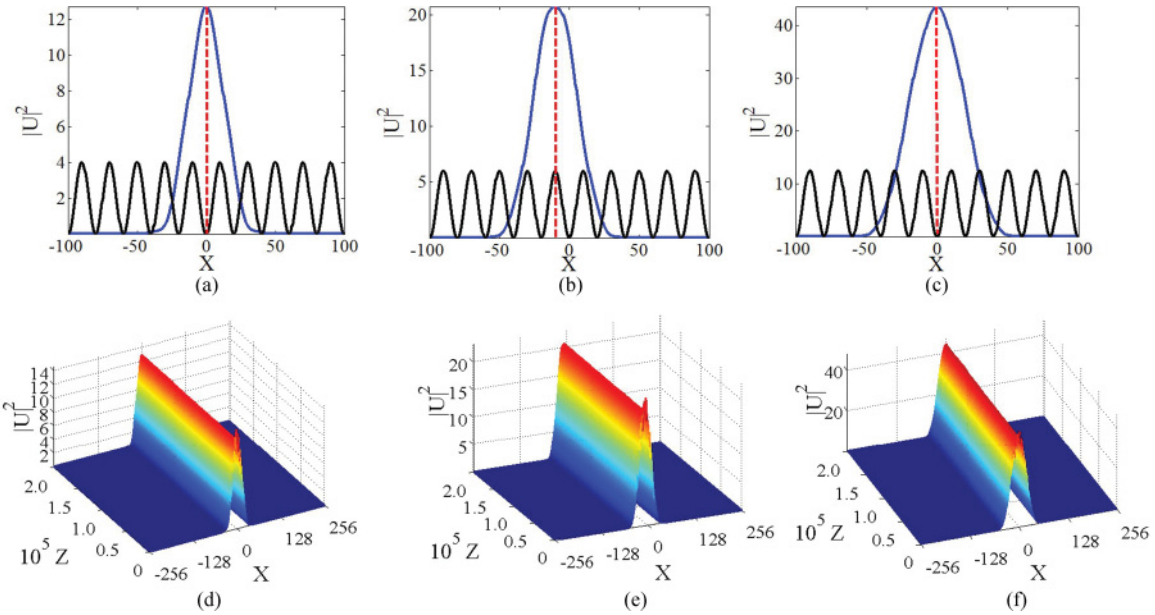

FIG. 2. (Color online) Numerically found soliton profiles (blue solid lines) for the modulation function (shown by the black solid line) with depth $V_0 = 0.02$ (recall the modulation period is scaled to be $d \equiv 20$). (a) At total power $P = 400$, the center of the soliton is located at the minimum of $V(x)$. (b) At $P = 800$, the soliton shifts to the maximum of $V(x)$. (c) At $P = 2000$, the solitons shifts back to the minimum of $V(x)$. Panels (d), (e), and (f) illustrate the stability of the solitons via direct simulations of their perturbed evolution.

where $U(x,P)$ is the soliton solution with power P. Using the integration in imaginary time, the data were collected for the solitons from $P = 100$ to 10000, with modulation depths $V_0 = 0.02, 0.03$, and 0.04. Real-time simulations of the evolution of these solutions in the framework of Eq. (2) demonstrate that they all are stable against perturbations.

Numerically found dependencies (4) are displayed in Fig. 3. The upper panels, Figs. 3 a–3(c), show that the soliton's center of mass switches (as said above) between the minimum ($x = 0$) and maximum ($x = -10$) of the modulation function $V(x)$. The period of the switching, ΔP, increases with the increase of modulation depth V_0. Further, Figs. 3(d)–3(f) show that the average width of the soliton grows with the increase of P and decrease of V_0.

B. Analytical approximations

In saturable nonlinear media, large-amplitude solitons are always broad. Accordingly, to develop an analytical approximation, we assume a soliton with the width much larger than d. Then, in the zero-order approximation, Eq. (2) is replaced by the equation with the averaged potential, $V(x) \to V_0/2$,

$$iu_z = -\frac{1}{2}u_{xx} + \frac{V_0}{2(1+|u|^2)}u. \tag{5}$$

Equation (5) gives rise to soliton solutions, $u(z,x) = e^{ikz}U(x-\xi)$, with the coordinate of the soliton's center ξ, and real function $U(y)$ obeying the following equation:

$$\frac{d^2U}{dy^2} = 2kU + \frac{V_0U}{1+U^2} \equiv -\frac{dW}{dU}, \tag{6}$$

where $y \equiv x - \xi$. The effective potential in Eq. (6),

$$W(U) = kU^2 + \frac{V_0}{2}\ln\left(\frac{1+U_0^2}{1+U^2}\right), \tag{7}$$

formally corresponds to the Newton's equation of motion for a particle with coordinate $U(y)$ (y plays the role of time) and unitary mass. Then, the shape of the soliton is determined by the respective energy equation,

$$\left(\frac{dU}{dy}\right)^2 + 2k\left(U_0^2 - U^2\right) + V_0\ln\left(\frac{1+U_0^2}{1+U^2}\right) = 0, \tag{8}$$

where U_0 is the amplitude of the soliton (the largest value of U). As usual, the soliton trajectory corresponds to the solution of Eq. (8) starting from $U = 0$ at $y = -\infty$, bouncing back from the potential well at $U = U_0$, $y = 0$, and returning to $U = 0$ at $y \to +\infty$. Setting in Eq. (8) $U = dU/dy = 0$, one can find a relation between k and U_0. Being interested in solutions with large amplitudes, we assume here $U_0^2 \gg 1$, which yields

$$k \approx -(V_0/2)U_0^{-2}\ln\left(U_0^2\right), \tag{9}$$

$$U_{\min}^2 \approx U_0^2/\ln\left(U_0^2\right), \tag{10}$$

$U_{\min}$ being the coordinate of the minimum of potential Eq. (7). Equation (10) implies $U_{\min}^2 \ll U_0^2$, i.e., the minimum of the potential is located much closer to $U = 0$ than the largest value U_0. This fact suggests a possibility to use the following approximation for solving Eq. (8): at the first stage of the approximation, we drop the logarithmic term in Eq. (8) altogether, i.e., we replace the equation by its "primitive version,"

$$\left(\frac{dU}{dy}\right)^2 + 2k\left(U_0^2 - U^2\right) = 0, \tag{11}$$

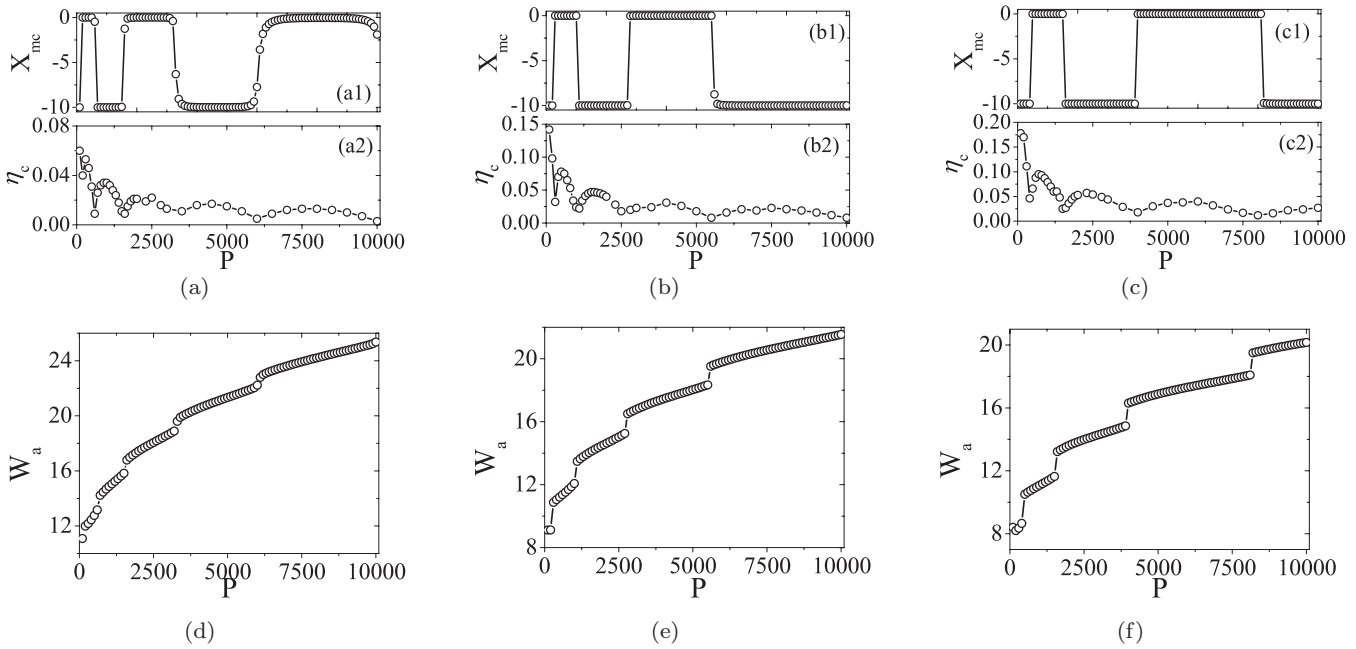

FIG. 3. (Color online) The plots in panels (a1)–(c1) display the coordinate of the soliton's center of mass, $X_{\rm mc}$, as a function of P, for $V_0 = 0.02, 0.03$, and 0.04, respectively. (a2)–(c2) display the critical kick that initiates the motion of the soliton, $\eta_{\rm c}$, as a function of P for $V_0 = 0.02, 0.03$, and 0.04. (d)–(f) The average width of the soliton as a function of P for $V_0 = 0.02, 0.03$, and 0.04.

whose obvious solution is

$$U(y) = U_0 \cos(\sqrt{-2k}\,y) \approx U_0 \cos\left(\frac{\sqrt{V_0 \ln\left(U_0^2\right)}}{U_0} y\right), \tag{12}$$

where Eq. (9) was used to replace k by the U_0.

At the second stage of the approximation, we recall that the particle does not perform periodic oscillations, as formally follows from Eq. (12), but it starts the motion from $U = 0$ at $y = -\infty$, and returns to $U = 0$ at $y \to +\infty$, as the soliton solution must do; see above. This means that approximation Eq. (12) is usable in interval

$$|y| < \frac{L_{\rm tot}}{2} \equiv \frac{\pi}{2\sqrt{-2k}} = \frac{\pi U_0}{2\sqrt{V_0 \ln\left(U_0^2\right)}}, \tag{13}$$

When the moving particle approaches edges of interval Eq. (13), the logarithmic term in Eq. (8), which was neglected in Eq. (11), "suddenly" becomes important, leading to the stoppage of the particle. Thus, the full approximation in the large-amplitude limit, $U_0 \gg 1$, amounts to representing the soliton as the QC:

$$U(y) \approx \begin{cases} U_0 \cos\left[\frac{\sqrt{V_0 \ln\left(U_0^2\right)}}{U_0} y\right], & \text{at} \quad |y| < L_{\rm tot}/2, \\ 0, & \text{at} \quad |y| > L_{\rm tot}/2, \end{cases} \tag{14}$$

where $L_{\rm tot}$, given by Eq. (13), plays the role of the total width of the QC. Note that the large amplitude U_0 of the soliton implies that the width [Eq. (13)] is also large, i.e., the QC is a sharply localized but wide localized pattern. In the present approximation, the total power of the soliton can be calculated as follows:

$$P \equiv \int_{-\infty}^{+\infty} |U(y)|^2 \, dy \approx \frac{1}{2} L_{\rm tot} U_0^2 = \frac{\pi U_0^3}{2\sqrt{V_0 \ln\left(U_0^2\right)}}. \tag{15}$$

Further, using the fact that P and U_0^2 are large, Eq. (15) can be approximately inverted, to give the peak power (squared amplitude) of the QC as a function of its total power:

$$U_0^2 \approx \left(\frac{2P}{\pi}\sqrt{\frac{2V_0}{3}(\ln P)}\right)^{2/3}. \tag{16}$$

Next, using Eq. (13), it is also possible to approximately express the full width of the compacton in terms of the total power:

$$L_{\rm tot} \approx \left(\frac{3\pi^2}{V_0}\frac{P}{\ln P}\right)^{1/3}. \tag{17}$$

Equations (16) and (17) are plotted in Fig. 4 for different values of P. In particular, Fig. 4(a) demonstrates that the analytical prediction for the peak power is consistent with the numerical results. On the other hand, the values of the width given by Eq. (17) [see Fig. 4(b)] are larger than their numerically found counterparts presented in Fig. 3(d). However, one should take into regard that width [Eq. (17)] is "all-inclusive" (total), while the width shown in Fig. 3(b) is the average one (definitely far smaller than the total width). Note also the similarity in the P-dependence of the width in Figs. 3(d) and 4(b).

To explain the position switchings of the QC, one may use the effective energy (potential) of the interaction of the QC with the spatial modulation, corresponding to the

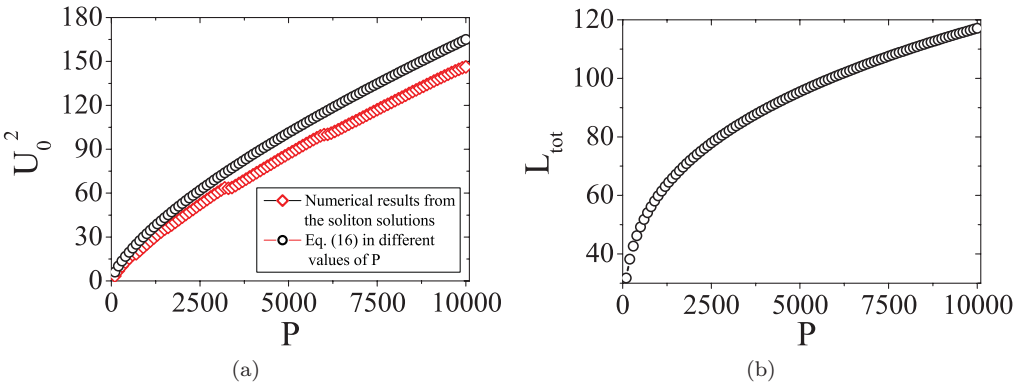

FIG. 4. (Color online) (a) The comparison of the numerical results for the peak power of the quasicompactons with the analytical prediction given by Eq. (16). (b) The full width of the quasicompacton, as predicted by Eq. (17). In this figure, $V_0 = 0.02$.

term $\sim \cos(2\pi x/d)$ in Eq. (3). This energy can be defined as follows, with regard to the definition of $y \equiv x - \xi$ in Eq. (6):

$$E_{\rm int}(\xi) = -V_0 \int_{-\infty}^{+\infty} dx \cos\left(\frac{2\pi x}{d}\right) \ln[1 + U^2(x)]$$
$$\approx -V_0 \int_{\xi - L_{\rm tot}/2}^{\xi + L_{\rm tot}/2} dx \cos\left(\frac{2\pi x}{d}\right) \ln[1 + U^2(x)]. \quad (18)$$

In this expression, it is taken into account that QC [Eq. (14)] occupies, approximately, a finite region of x, $\xi - L_{\rm tot}/2 < x < \xi + L_{\rm tot}/2$. After three integrations by parts, Eq. (18) can be approximately calculated as follows:

$$E_{\rm int}(\xi) \approx K_d \ln\left(U_0^2\right) \sin\left[\frac{\pi^2 U_0}{d\sqrt{V_0 \ln\left(U_0^2\right)}}\right] \cos\left(\frac{2\pi}{d}\xi\right), \quad (19)$$

where $K_d \equiv V_0^2 d^3/\pi^3$. Equation (19) predicts that the minimum of the interaction energy is located at points $\xi = nd$ with integer n (at minima of the modulation function) for values of U_0 such that $\sin\{\pi^2 U_0/[d\sqrt{V_0 \ln(U_0^2)}]\} < 0$, and at points $\xi = (n + 1/2)d$ (at maxima of the modulation) in the opposite case, $\sin\{\pi^2 U_0/[d\sqrt{V_0 \ln(U_0^2)}]\} > 0$. Because U_0 grows as the function of P, as per Eq. (16), this means that, with the increase of P, the position of the energy minimum must indeed switch between adjacent extrema of the modulation function. The fact that V_0 appears in the denominator of the argument of the sinusoidal factor explains why the period of the switching increases with V_0.

III. MOBILITY OF THE QUASICOMPACTONS

A. Driving the soliton by the phase tilt

Mobility of solitons under the combined action of LL and NL is a problem that was considered in a number of different settings [2,26–29]. To set the QC in motion, we follow the standard approach, suddenly kicking a quiescent one, i.e., multiplying the respective solution, $U(x)$, by the phase-tilt factor: $U(x,\eta) \to \exp(i\eta x)U(x)$, where η is the strength of kick.

The simulated propagation of the QC, induced by kicking the standing one, $U(x, P = 2000)$, is displayed in Fig. 5, for two different values of η. It is observed that $\eta = 0.020(\pi/d)$ causes only oscillations of the soliton, without any progressive motion. However, a slightly higher kick, $\eta = 0.025(\pi/d)$, is sufficient to set the same soliton in persistent motion. These results imply that there must be a threshold (critical) value of the kick, η_c, such that the kick with $\eta > \eta_c$ makes the given QC a traveling soliton. For $P = 2000$, it is $\eta_c = 0.021(\pi/d)$.

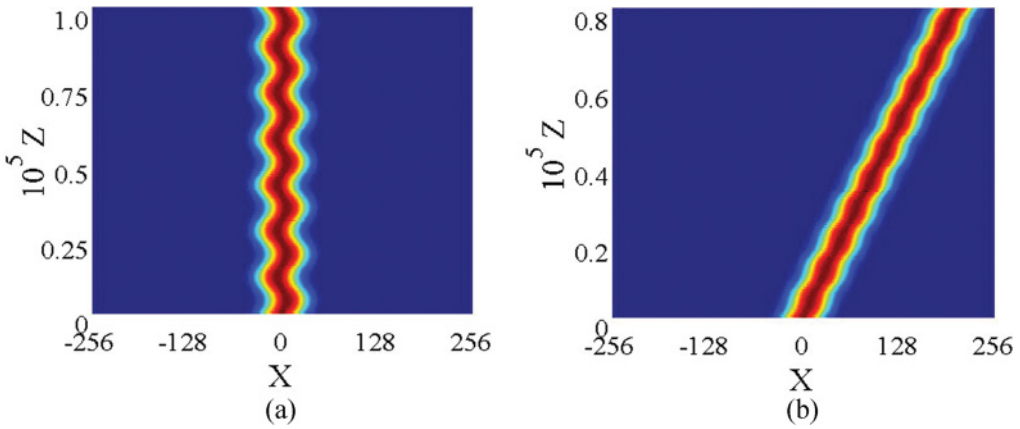

FIG. 5. (Color online) Direct simulations of the compacton with $P = 2000$, initiated by the application of the phase tilt with $\eta = 0.020(\pi/d)$ (a) and $\eta = 0.025(\pi/d)$ (b). The lattice depth is $V_0 = 0.02$.

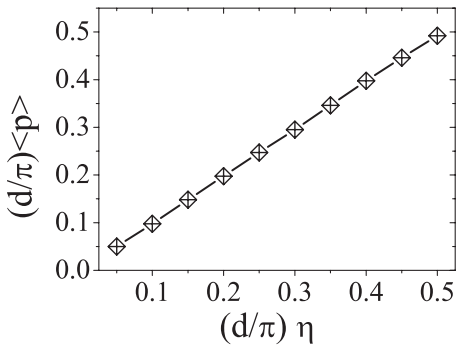

FIG. 6. The momentum of the soliton with $P = 2000$, measured at $z = 1000$, as a function of initial kick η.

The critical kick for the QCs is shown as a function of the total power in Figs. 3(a)–3(c), for $V_0 = 0.02, 0.03$, and 0.04. The general trend to the decrease of η_c with the increase of P is explained by the broadening of the soliton with the increase of the total power in the case of the saturable nonlinearity and ensuing enhancement of the solitons' mobility [29]. A specific feature of the INPC is that oscillations of η_c are superimposed on top of the gradual decay of the critical kick, the period of the oscillations coinciding with that of the switching of the center-of-mass position. Figures 3(a)–3(c) also demonstrate that η_c decreases with the decreases of modulation depth V_0. The latter trend is correlated with the fact that, as seen in Figs. 3(d)–3(f), the width of the solitons increases, making them more mobile, with the decrease of V_0 (as well as with the increase of P).

Further, Fig. 6 shows that the momentum of the moving soliton, which is defined as

$$\langle p(z)\rangle = -i \int dx U(x,z,\eta)^* U_x(x,z,\eta), \tag{20}$$

is, naturally, a linear function of the initial kick, η. Further simulations (not shown here) demonstrate that the QC are *not* destroyed even by a very strong kick, far exceeding η_c.

It is relevant to compare the mobility of large-amplitude solitons in the INPCs models with the saturable and cubic self-focusing. In the latter case, Eq. (2) is replaced by [4]

$$iu_z = -\tfrac{1}{2}u_{xx} + V(x)(1 - |u|^2)u, \tag{21}$$

where we chose the modulation function, $V(x)$, in the same form as in Eq. (3), with $V_0 = 0.02$ and $d = 20$. A typical example of simulations of the mobility of solitons in this model is displayed in 7(a)–7(c), for three kicks, $\eta = 0.15\pi/d, 0.25\pi/d$, and $0.35\pi/d$. In particular, Fig. 7(a) shows that $\eta = 0.15\pi/d$ give rise to oscillations of the soliton, without depinning. Further, it is observed in Fig. 7(b) that the

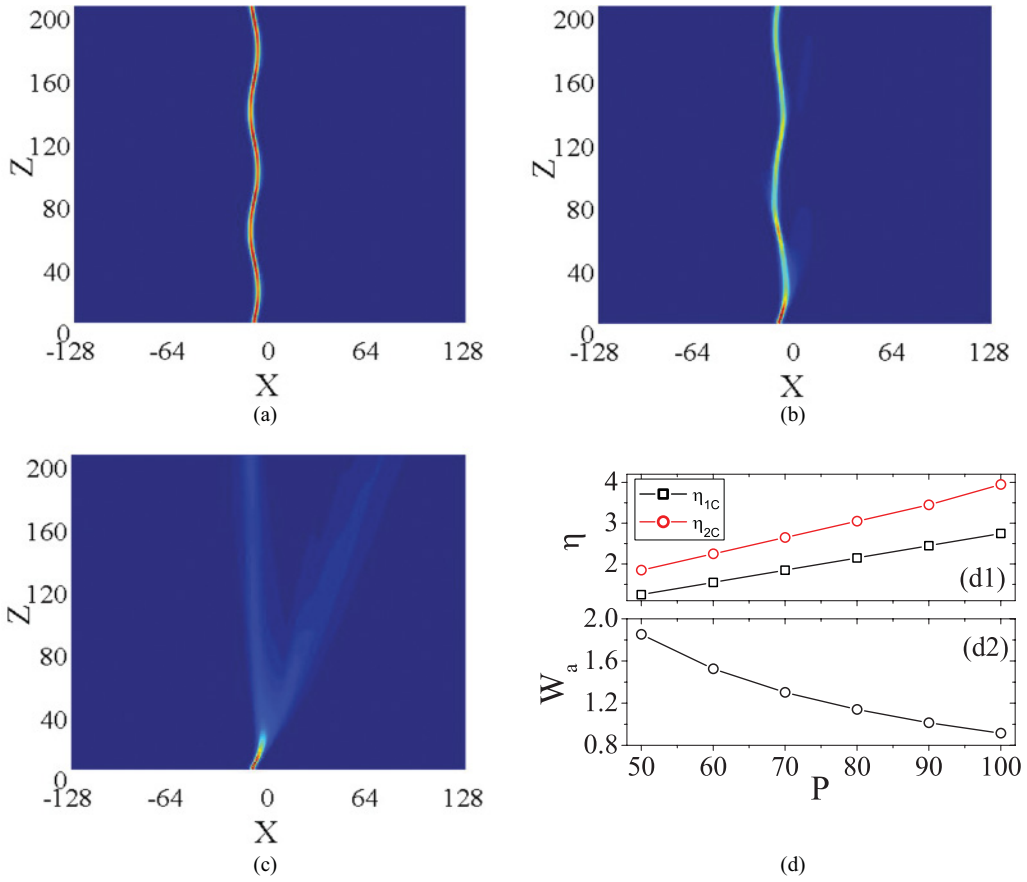

FIG. 7. (Color online) (a) Direct simulations of the evolution of the soliton with total power $P = 80$ in the model with the cubic nonlinearity [Eq. (21)], initiated by the kick with strengths $\eta = 0.15(\pi/d)$ (a), $0.25(\pi/d)$ (b), and $\eta = 0.35(\pi/d)$ (c). (d) The top plot: η_{1c} is the border between stable solitons and fuzzy beams; η_{2c} is the border between the fuzzy beams and completely destroyed ones. The bottom plot shows the average width of the quiescent soliton versus its total power P.

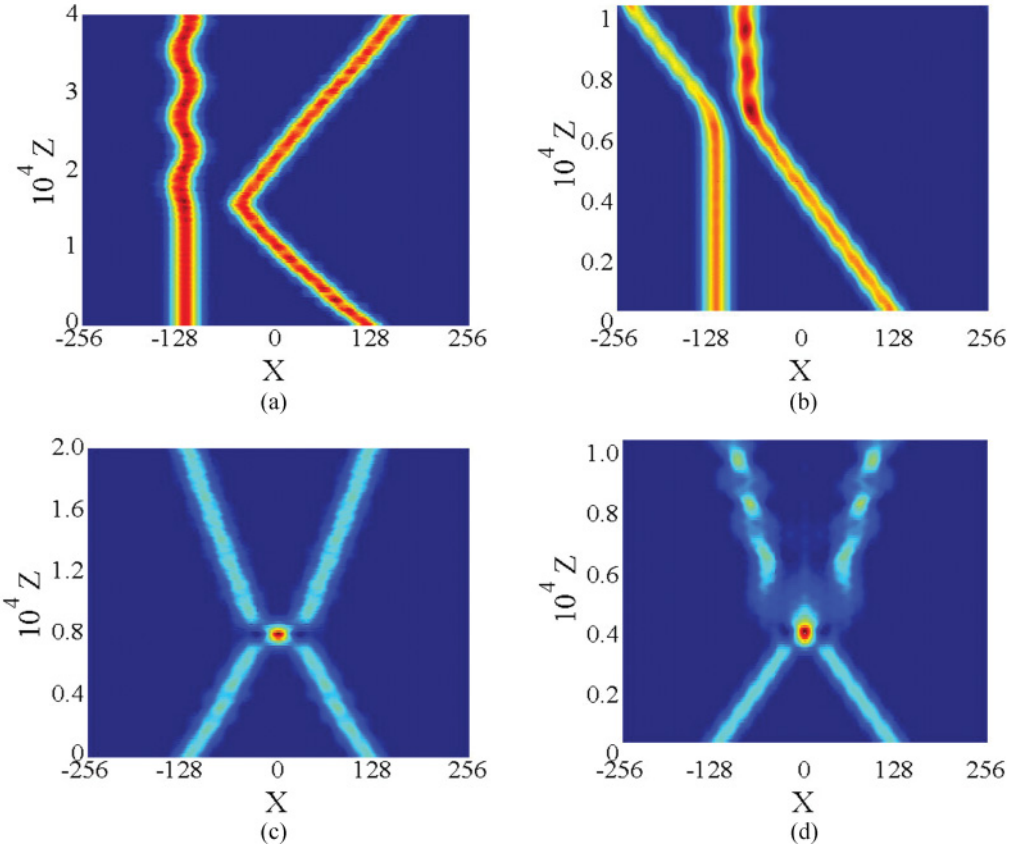

FIG. 8. (Color online) Direct simulation of the collisions initiated by kicks $\eta_1 = 0$, $\eta_2 = 0.1(\pi/d)$ (a); $\eta_1 = 0$, $\eta_2 = 0.2(\pi/d)$ (b); $\eta_1 = 0.1(\pi/d)$, $\eta_2 = 0.1(\pi/d)$ (c); $\eta_1 = 0.2(\pi/d)$, $\eta_2 = 0.2(\pi/d)$ (d). Other parameters are $P = 400$, $x_0 = 120$, and $V_0 = 0.02$. As in the rest of the paper, the scaling is fixed by $d \equiv 20$.

stronger kick, $\eta = 0.25\pi/d$, transforms the soliton into an oscillatory beam with a fuzzy shape, but, still, it was not set in motion. Finally, Fig. 7(c) demonstrates that the strongest kick, $\eta = 0.35\pi/d$, completely destroys the soliton (recall the destruction never happens in the model with the saturable nonlinearity). Therefore, there must exist critical values of the kick separating the stable solitons, fuzzy beams, and complete destruction. These borders are plotted in the top panel of Fig. 7(d), in the range of powers $50 < P < 100$ (the average width of the static soliton in the same region is plotted, versus P, in the bottom panel). Thus, the large-amplitude solitons in the INPC model with the cubic self-focusing are not mobile at all. On the other hand, dynamics of small-amplitude solitons in the models with the saturable and cubic nonlinearities are similar, due to the obvious expansion, $(1 + |u|^2)^{-1} \approx 1 - |u|^2$ (results for this case are not shown here in detail, as they are less interesting).

B. Collisions between moving quasicompactons

Collisions are a natural way to test interactions between solitons. Here we present some numerical results for collisions between QCs in the INPC with the saturable nonlinearity. The initial state at $z = 0$ is taken as a set of two far-separated kicked solitons:

$$u(x) = U(x + x_0, P)e^{i\eta_1(x+x_0)} + U(x - x_0, P)e^{-i\eta_2(x-x_0)}, \quad (22)$$

where $U(x \pm x_0, P)$ are the QC pulses with power P, which are centered at $x = \mp x_0$, and $\eta_{1,2}$ are the kicks applied to them. Simulations of Eq. (2) with initial conditions Eq. (22) are displayed in Fig. 8.

The simulations demonstrate the repulsive interaction between the colliding QC. In Figs. 8(a) and 8(b), they bounce back without overlapping, because the collision velocity is small [nevertheless, one of the solitons suffers a conspicuous perturbation in Fig. 8(a)]. In Figs. 8(c) and 8(d), the larger velocities give rise to the overlap between the colliding QCs, which results in the strong inelasticity of the collision in the case displayed in Fig. 8(d).

IV. CONCLUSIONS

The objective of this work was to consider 1D solitons in the INPC (inverted nonlinear photonic crystal) with competing LL and NL (linear and nonlinear lattices). Unlike recently studied models with the cubic nonlinearity, we here consider the saturable self-focusing. The 1D crystal of this type was recently fabricated, using the SU-8 polymer material periodically doped with Rhodamine-B, which lends the medium the saturable nonlinearity. Combining numerical methods and analytical approximations, we have demonstrated that broad solitons are sharply localized in this setting, thus taking the shape of the QCs. With the increase of the total power, P, the QC remains a stable object, which switches its position

between the linear and nonlinear layers, which form the INPC. The width of the soliton increases with P, which is a manifestation of the saturable nonlinearity. The large width of the QC makes it a mobile object, unlike solitons in the INPC with the cubic nonlinearity. The threshold value of the transverse kick (phase tilt), which is necessary to set the QC in motion, was found as a function of P. The threshold value gradually decays with the increase of P. Collisions between two moving QCs were also studied, by means of direct simulations.

The results reported in this work may be applied to the design of all-optical data-processing schemes. In particular, the power-controlled switch of the spatial soliton between adjacent layers, as well as the high mobility of these solitons, may be quite relevant properties, in this context.

This work may be extended in other directions. It particular, 2D waveguide arrays, based on the RhB–SU-8 mixtures, can be fabricated [21,22], which suggests considering spatial solitons in two-dimensional INPC with the saturable nonlinearity.

ACKNOWLEDGMENTS

Y.L. appreciates useful discussions with Dr. M. Feng. This work was supported by the Chinese agencies NKBRSF (Grant No. G2010CB923204), NSFC (Grant No. 11104083), and CNNSF (Grant No. 10934011).

[1] Q. Li, C. T. Chan, K. M. Ho, and C. M. Soukoulis, Phys. Rev. B **53**, 15577 (1996); E. Lidorikis, Q. Li, and C. M. Soukoulis, *ibid.* **54**, 10249 (1996); D. Hennig and G. P. Tsironis, Phys. Rep. **307**, 333 (1999); B. Maes, P. Bienstman, and R. Baets, J. Opt. Soc. Am. B **22**, 613 (2005).

[2] Y. V. Kartashov, B. A. Malomed, and L. Torner, Rev. Mod. Phys. **83**, 247 (2011).

[3] A. A. Sukhorukov and Y. S. Kivshar, Phys. Rev. Lett. **87**, 083901 (2001); Y. Kominis and K. Hizanidis, Opt. Lett. **31**, 2888 (2006); Y. Kominis, Phys. Rev. E **73**, 066619 (2006); Y. Kominis and K. Hizanidis, Opt. Exp. **16**, 12124 (2008); Z. Rapti, P. G. Kevrekidis, V. V. Konotop, and C. K. R. T. Jones, J. Phys. A **40**, 14151 (2007).

[4] T. Mayteevarunyoo and B. A. Malomed, J. Opt. Soc. Am. B **25**, 1854 (2008).

[5] P. Xie, Z.-Q. Zhang, and X. Zhang, Phys. Rev. E **67**, 026607 (2003); A. Ferrando, M. Zacarés, P. F. de Córdoba, D. Binosi, and J. A. Monsoriu, Opt. Exp. **11**, 452 (2003).

[6] H. L. F. da Luz, F. Kh. Abdullaev, A. Gammal, M. Salerno, and L. Tomio, Phys. Rev. A **82**, 043618 (2010).

[7] A. Ferrando, M. Zacarés, P. F. de Córdoba, D. Binosi, and J. A. Monsoriu, Opt. Exp. **12**, 817 (2004); Y. V. Kartashov, A. Ferrando, A. A. Egorov, and L. Torner, Phys. Rev. Lett. **95**, 123902 (2005).

[8] P. St. J. Russell, J. Lightwave Tech. **24**, 4729 (2006); S. Arismar Cerqueira, Jr., Rep. Prog. Phys. **73**, 024401 (2010).

[9] J. D. Joannopoulos, S. G. Johnson, J. N. Winn, and R. D. Meade, *Photonic Crystals: Molding the Flow of Light* (Princeton University Press, Princeton, 2008); M. Skorobogatiy and J. Yang, *Fundamentals of Photonic Crystals Guiding* (Cambridge University Press, Cambridge, 2009).

[10] L. C. Qian, M. L. Wall, S. Zhang, Z. Zhou, and H. Pu, Phys. Rev. A **77**, 013611 (2008); T. Mayteevarunyoo, B. A. Malomed, and G. Dong, *ibid.* **78**, 053601 (2008).

[11] F. Luan, A. K. George, T. D. Hedley, G. J. Pearce, D. M. Bird, J. C. Knight, and P. St. J. Russell, Opt. Lett. **29**, 2369 (2004); G. Bouwmans, L. Bigot, Y. Quiquempois, F. Lopez, L. Provino, and M. Douay, Opt. Exp. **13**, 8452 (2005); A. Fuerbach, P. Steinvurzel, J. A. Bolger, A. Nulsen, and B. J. Eggleton, Opt. Lett. **30**, 830 (2005).

[12] T. T. Larsen, A. Bjarklev, D. S. Hermann, and J. Broeng, Opt. Exp. **11**, 2589 (2003); F. Du, Y. Q. Lu, and S. T. Wu, Appl. Phys. Lett. **85**, 2181 (2004); M. W. Haakestad, T. T. Alkeskjold, M. D. Nielsen, L. Scolari, J. Riishede, H. E. Engan, and A. Bjarklev, IEEE Phot. Tech. Lett. **17**, 819 (2005); C. R. Rosberg, F. H. Bennet, D. N. Neshev, P. D. Rasmussen, O. Bang, W. Królikowski, A. Bjarklev, and Y. S. Kivshar, Opt. Exp. **15**, 12145 (2007).

[13] D. Jaksch, C. Bruder, J. I. Cirac, C. W. Gardiner, and P. Zoller, Phys. Rev. Lett. **81**, 3108 (1998); M. Greiner, O. Mandel, T. Esslinger, T. W. Hansch, and I. Bloch, Nature (London) **415**, 39 (2002).

[14] S. Ghanbari, T. D. Kieu, A. Sidorov, and P. Hannaford, J. Phys. B **39**, 847 (2006).

[15] S. Inouye, M. R. Andrews, J. Stenger, H. J. Miesner, D. M. Stamper-Kurn, and W. Ketterle, Nature (London) **392**, 151 (1998); S. L. Cornish, N. R. Claussen, J. L. Roberts, E. A. Cornell, and C. E. Wieman, Phys. Rev. Lett. **85**, 1795 (2000); E. Timmermans, P. Tommasini, M. S. Hussein, and A. Kerman, Phys. Rep. **315**, 199 (1999).

[16] P. O. Fedichev, Y. Kagan, G. V. Shlyapnikov, and J. T. M. Walraven, Phys. Rev. Lett. **77**, 2913 (1996); M. Theis, G. Thalhammer, K. Winkler, M. Hellwig, G. Ruff, R. Grimm, and J. H. Denschlag, *ibid.* **93**, 123001 (2004).

[17] Y. V. Kartashov, V. A. Vysloukh, and L. Torner, Opt. Lett. **33**, 1747 (2008); **33**, 2173 (2008).

[18] Y. Li, B. A. Malomed, M. Feng, and J. Zhou, Phys. Rev. A **82**, 063813 (2010); C. Hang and V. V. Konotop, *ibid.* **81**, 053849 (2010).

[19] X. Q. Jiang, B. Zhang, Z. W. Lu, and X. D. Sun, Phys. Rev. A , **83**, 053823 (2011); J. Wu, M. Feng, W. Pang, S. Fu, and Y. Li, J. Nonlinear Opt. Phys. **20**, 193 (2011).

[20] A. Szameit, J. Burghoff, T. Pertsch, S. Nolte, A. Tünnermann, and F. Lederer, Opt. Exp. **14**, 6055 (2006); D. Blömer, A. Szameit, F. Dreisow, T. Pertsch, S. Nolte, and A. Tünnermann, *ibid.* **14**, 2151 (2006).

[21] M. Feng, Y. Liu, Y. Li, X. Xie, and J. Zhou, Opt. Exp. **19**, 7222 (2011).

[22] J. Li, B. Liang, Y. Liu, P. Zhang, J. Zhou, S. O. Klimonsky, A. S. Slesarev, Y. D. Tretyakov, L. O'Faolain, and T. F. Krauss, Adv. Mater. **22**, 1 (2010).

[23] M. L. Chiofalo, S. Succi, and M. P. Tosi, Phys. Rev. E **62**, 7438 (2000); J. Yang, and T. I. Lakoba, Stud. Appl. Math. **120**, 265 (2008); **118**, 153 (2007); Y. Li, W. Pang, Y. Chen, Z. Yu, J. Zhou, and H. Zhang, Phys. Rev. A **80**, 043824 (2009).
[24] P. Rosenau and J. M. Hyman, Phys. Rev. Lett. **70**, 564 (1993).
[25] J. He and X. Wu, Chaos Sol. Fractals **29**, 108 (2006).
[26] H. Sakaguchi, and B. A. Malomed, Phys. Rev. E **70**, 066613 (2004).
[27] J. Zhou, C. Xue, Y. Qi, and S. Lou, Phys. Lett. A **372**, 4395 (2008).
[28] Y. V. Kartashov, V. A. Vysloukh, and L. Torner, Prog. Opt. **52**, 63 (2009).
[29] M. Öster, M. Johansson, and A. Eriksson, Phys. Rev. E **67**, 056606 (2003); R. A. Vicencio and M. Johansson, *ibid.* **73**, 046602 (2006); R. Botet and H. Kuratsuji, *ibid.* **83**, 036602 (2011).